Journal of Microscopy, Vol. 221, Pt 1 January 2006, pp. 1–7
Received 11 August 2005; accepted 20 October 2005

SHORT COMMUNICATION

An approach to the systematic distortion correction in aberration-corrected HAADF images

A. M. SANCHEZ*†, P. L. GALINDO‡, S. KRET§, M. FALKE¶, R. BEANLAND** & P. J. GOODHEW†

Departamento de Ciencia de los Materiales e I.M. y Q.I., and ‡Departamento de Lenguajes y Sistemas Informaticos, Universidad de Cadiz, Puerto Real, 11510, Spain

†Department of Engineering, University of Liverpool, Liverpool L69 3GH, U.K.

§Institute of Physics, Polish Academy of Science, Al. Lotnikow 32/46. PL-020668 Warzawa, Poland

¶UK SuperSTEM, Daresbury Laboratory, Daresbury WA4 4AD, U.K.

***Bookham Technology, Caswell, Towcester, Northants. NN12 8EQ, U.K.*

Key words. Algorithm, distortion, HAADF, nanostructures, STEM.

Summary

Systematic distortion has been analysed in high-angle annular dark-field (HAADF) images which may be caused by electrical interference. Strain mapping techniques have been applied to a strain-free GaAs substrate in order to provide a broad analysis of the influence of this distortion on the determination of local strain in the heterostructure. We have developed a methodology for estimating the systematic distortion, and we correct the original images by using an algorithm that removes this systematic distortion.

Introduction

Quantitative measurement of internal strain at an atomic spatial resolution, based on the analysis of conventional high-resolution transmission electron microscopy (HRTEM) images, has become a powerful technique which can be used in a variety of materials systems (Rosenauer *et al.*, 1997; Hÿtch & Plamann, 2001; Kret *et al.*, 2001). The distance between adjacent atom columns in an HRTEM image can be measured – usually to an accuracy better than 1% – using methodologies applied in real (Rosenauer *et al.*, 1997; Bierwolf *et al.*, 1993; Kret *et al.*, 2001) or Fourier space (Hÿtch *et al.*, 1998). However, the interpretation of HRTEM images is not always straightforward and considerations due to the sample thickness and defocus conditions should be taken into account. High-angle annular dark-field (HAADF) scanning transmission electron microscopy (STEM) can be applied in a similar way to HRTEM, i.e. to produce high-resolution images of the atomic columns of a crystalline material. One of the most important advantages of this imaging technique is that it does not show contrast reversal with specimen thickness and microscope defocus. Furthermore, whereas HRTEM has to be performed in a very thin area of the sample (5–10 nm), HAADF images can be obtained from thicker areas.

The spherical aberration of the objective lens, C_s, in the transmission electron microscope is one of the main parameters which limits spatial resolution. Recent developments using a set of quadrupole and octupole lenses (Krivanek *et al.*, 1999) in dedicated STEM microscopes have allowed the spherical aberration to be corrected, giving electron beams with sub-Angstrom dimensions. This significantly increases the range of materials from which high-resolution images can be obtained in this type of microscope.

An artefact common to all microscopes that use a scanning electron beam is the presence of small beam deflections due to external electromagnetic fields, as well as hysteresis effects during the 'fly back' between scan lines. These artefacts can be disastrous if the precise location of an atom column is to be determined with subpixel accuracy. Fortunately, the majority of these image distortions are time-invariant, i.e. they are essentially the same in all images obtained under the same conditions. We call these distortions 'systematic' (as opposed to those that vary randomly with time, which are 'non-systematic'). Here we describe the measurement of systematic distortions in high-resolution images obtained from an aberration-corrected dedicated STEM, using high-resolution

Correspondence to: Dr A. Sanchez. Fax: +34 956 016288; e-mail: ana.fuentes@uca.es

[110] images of strain-free GaAs. There are a number of different algorithms for strain mapping, any of which could be appropriate for this task, given that the analysed material showed no dislocations or defects. We then show that a simple but effective way to reconstruct the non-distorted image can be used to allow quantitative analysis of strain in HAADF images with atomic-scale spatial resolution.

Materials and methods

Cross-section TEM specimens of an InAs/GaAs heterostructure on a (001) GaAs substrate were prepared as described in Beanland (2003). The material was backthinned to approximately 100 μm thickeness and a small piece was cleaved and mounted on a support grid. This was mechanically thinned to approximately 20 μm and polished using a 1-μm diamond suspension on a soft nap pad. The specimens were ion-milled to electron transparency using Ar^+ ions at 6 kV and a beam incidence angle of 3° (uncooled). A final low-energy 'clean' of the sample at 2 kV was employed to minimize amorphous surface layers. Investigations were carried out using a VG HB501 UX FEG-STEM equipped with the recently developed Nion spherical aberration corrector operating at 100 kV.

Two algorithms for strain mapping were used, Geometric Phase (Hÿtch & Plamann, 2001) and Peak Pairs (Galindo *et al*., 2005). The Geometric Phase algorithm works in Fourier space, and calculates the displacement field by combining information from two lattice periodicities, i.e. the phase images for two different and non-collinear vectors. By contrast, Peak Pairs works in real space and has been shown to give similar results to Geometric Phase in most cases. When using the Geometric Phase algorithm, problems may arise when phase images contain $[-\pi, \pi]$ boundaries, as the 'unwrapping' problem is not yet completely solved. This gives errors in the determination of displacement and strains, which propagate to the final image reconstruction (Hÿtch & Plamann, 2001). By contrast, Peak Pairs works in real space, avoiding the unwrapping problem. Because the HAADF images of unstrained material that we have used do not have $[-\pi, \pi]$ phase boundaries, we have been able to use the Geometric Phase methodology without problems.

Our initial approach was to apply the Geometric Phase algorithm to HAADF images of unstrained GaAs viewed along [110]. The displacement field was calculated by the combination of information from two lattice periodicities from the phase images for two different and non-collinear $\mathbf{g}_{111}$ vectors (g_1 and g_2, respectively),

$$\begin{pmatrix} P_{g_1} \\ P_{g_2} \end{pmatrix} = -2\pi \begin{pmatrix} g_{1x} & g_{1y} \\ g_{2x} & g_{2y}y \end{pmatrix} \begin{pmatrix} u_x \\ u_y \end{pmatrix}$$

where P_g is the phase image, g_x and g_y the k_x and k_y components of the vector g and u_x and u_y are the x and y components of the displacement field at position $r = (x, y)$.

Next, the systematic lattice distortion tensor β_{ij} was calculated as the numerical derivative of the displacement field (Hÿtch & Plamann, 2001; Kret *et al*., 2001),

$$\beta_{ij} = \begin{pmatrix} \beta_{xx} & \beta_{xy} \\ \beta_{yx} & \beta_{yy} \end{pmatrix} = \begin{pmatrix} \partial u_x / \partial x & \partial u_x / \partial y \\ \partial u_y / \partial x & \partial u_y / \partial y \end{pmatrix}.$$

The resulting maps of the different strain components β_{ij} were then used to determine the nature of the systematic distortions. It was found that only the component β_{yx} showed strong systematic variations, and even in this case there was essentially no variation along the y-axis. We thus took the average ρ_{yx}^{sys} of all values of β_{yx} in each column in the image, as follows:

$$\rho_{yx}^{sys}(i) = \frac{1}{N} \sum_{j=1}^{N} \beta_{yx}(i, j) \quad i = 1 \ldots M \tag{1a}$$

where M and N are the number of pixels. The systematic distortion (β_{yx}^{sys}) along the x-axis is thus

$$\beta_{yx}^{sys}(i, j) = \rho_{yx}^{sys}(i), \quad i = 1 \ldots M, \quad j = 1 \ldots N. \tag{1b}$$

From this systematic distortion, the corresponding displacement for each pixel was calculated, in both x and y, as follows. By definition,

$$\beta_{yx}^{sys} = \frac{\partial u_y^{sys}}{\partial x}. \tag{2}$$

Given that one pixel is the smallest spatial unit in the image, we may approximate

$$\beta_{yx}^{sys}(i, j) = \frac{\partial u_y^{sys}}{\partial x} \approx u_y^{sys}(i, j) - u_y^{sys}(i-1, j). \tag{3}$$

Hence,

$$u_y^{sys}(i, j) \approx \beta_{yx}^{sys}(i, j) + u_y^{sys}(i-1, j) \tag{4}$$

and

$$u_y^{sys}(i, j) = u_y^{sys}(0, j) + \sum_{k=1}^{n} \beta_{yx}^{sys}(i-k, j). \tag{5}$$

Similarly, given that there is no systematic distortion along x,

$$u_y^{sys}(0, j) = u_y^{sys}(0, 0) + \sum_{k=1}^{m} \beta_{xy}^{sys}(0, j-k) = u_y^{sys}(0, 0). \tag{6}$$

Imposing the restriction $u_y^{sys}(0, 0) = 0$, we obtain the systematic displacements from the systematic distortions

$$u_y^{sys}(i, j) = u_y^{sys}(0, j) + \sum_{k=1}^{n} \beta_{yx}^{sys}(i-k, j) = \sum_{k=1}^{n} \beta_{yx}^{sys}(i-k, j). \tag{7}$$

This restriction does not affect the final result. In fact, we may assign any constant value to $u_y^{sys}(0, 0)$, and the only difference in the resulting image will be a vertical shift.

These displacements allow us to produce an image in which pixels have intensities $I^*(i, j)$ corresponding to the intensity in the original image I if there was no systematic distortion, i.e.

$$I^*(i, j) = I(i, j - u_y^{sys}(i, j)). \quad (8)$$

However, the calculated displacements (u_{yx}^{sys}) are non-integers, and some interpolation is necessary in order to evaluate the intensity of the image at non-integer positions. In our experiments, we used linear interpolation between adjacent values in the y-direction of the image ($I(i, floor(j - u_y^{sys}(i, j)))$ and $I(i, ceil(j - u_y^{sys}(i, j)))$) (*floor* and *ceil* functions round their argument down and up to the next integer, respectively), but other approaches such as cubic interpolation could be applied.

Results and discussion

An exhaustive analysis of the systematic distortion in relaxed areas of GaAs has been carried out. The precision in the scanning process has been analysed using strain mapping methodologies applied to non-distorted GaAs, as an internal reference. In this way, the distortions in the x and y scanning directions can be determined. All the STEM images were recorded under the same conditions, with 50-Hz line synchronization. The 'fly back' time was also adjusted so that it would not affect the images. Using scan rotation, the crystal and microscope coordinate systems were aligned, with the growth direction close to parallel to the y-axis. Sets of HAADF images were recorded from several areas corresponding to the GaAs substrate at different magnifications and scan times. Figure 1 shows HAADF images of the non-distorted GaAs substrate with the beam parallel to the [110] axis, with an image size of 1024×1024 and magnification of 0.04170 nm pixel^{-1} (Fig. 1a) and 0.02087 nm pixel^{-1} (Fig. 1b), indicated magnification 500 000 and 1 000 000×, respectively. A bending of the lattice planes is present in both images. In order to determine the precision in the scanning process, a set of images at 1 000 000 and 500 000×, recorded at different times, has been analysed using the strain mapping technique.

The main result of the strain mapping analysis is that the y-component of the displacement changes with the x-coordinate, which produces 'waves' in the lines of atomic columns. By contrast, the x-component of the displacement was not strongly affected by the systematic distortion. This phenomenon is well illustrated in Fig. 2(a,b), showing the displacement fields u_x and u_y. The displacement component in the y direction, u_y, is responsible for the light and dark vertical bands. This banded pattern originates in the slight movement of the beam during each scanned line, possibly (but not necessarily) due to 50-Hz noise. The band patterns observed in u_y are equally visible on the map of the derivative of the displacement (β_{yx}) (Fig. 2c) but they do not appear in the β_{yy} map (Fig. 2d). This allows us to conclude even when there is a shift of the columns of pixels in the y direction, the periodicity of the GaAs crystal is preserved in the y direction. This means that the GaAs substrate can be taken as a reference image, which allows tetragonal distortion to be calculated, even for uncorrected images. The wider applicability of this approach is not known at present, as it is likely that each microscope has its own unique distortion field.

It is also interesting to analyse how artificial distortion changes with time and magnification. Figure 3 shows β_{yx} in four 1 000 000× HAADF images (Fig. 3a–d) and two 500 000× images (Fig. 3e,f). In Fig. 3(a)–(d) vertical stripes of almost constant vertical displacement can be observed. The systematic distortion at 1 000 000× magnification is relatively constant with time, as the same pattern of stripes appears in each image. The same distortion pattern appears again in the images recorded at 500 000×. The comparison between Fig. 3(c,e) shows that β_{yx} fluctuates less at this magnification than at 1 000 000×.

Figure 4 shows a plot of β_{yx} averaged along the y-axis for six different images, four of them recorded at 1 000 000× and two others at 500 000×. The two uppermost profiles, corresponding

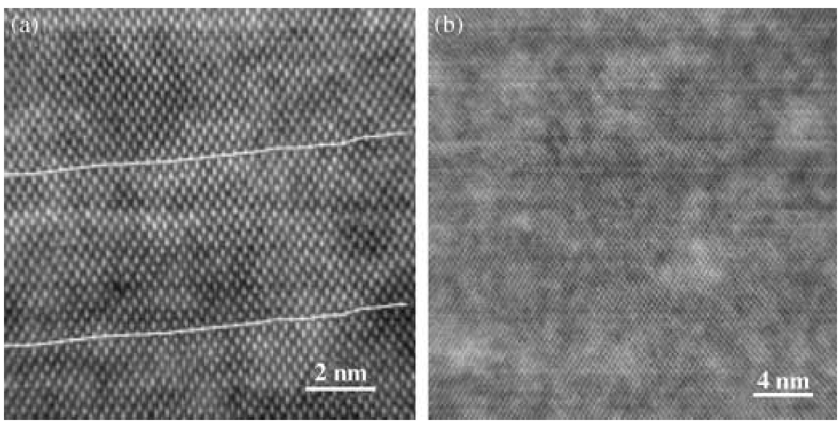

Fig. 1. High-angle annular dark-field images of unstrained GaAs viewed along [110], recorded at (a) 1 000 000× and (b) 500 000×. Two white lines were drawn to highlight the lattice plane bending.

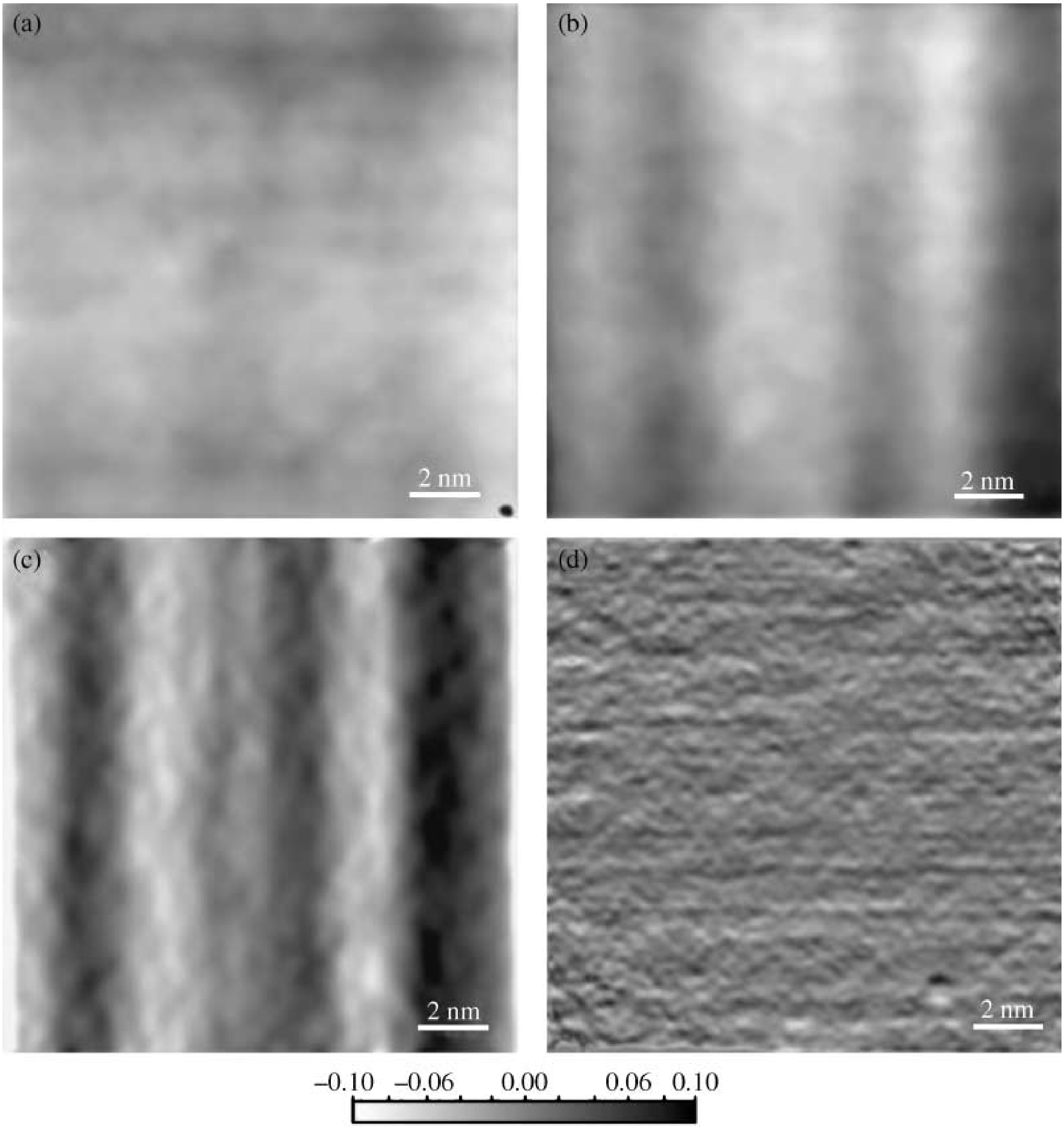

Fig. 2. (a) u_x and (b) u_y displacement components. u_y shows a banded pattern. (c) The β_{yx} component of the distortion tensor. The banded pattern is clear. (d) The β_{yy} component, with no banded pattern. Note that the scale is for β_{yx} and β_{yy}, and not for displacement.

to images recorded at 500 000×, have been multiplied by a factor of 2. The same pattern is present in all the profiles, so we may conclude that the banded pattern is essentially constant in shape, while its amplitude changes in proportion to the magnification. This has been used to correct the images and remove the systematic deformation following the methodology described in the Materials and methods section. Figure 5(a,b) shows the corrected images, at 1 000 000× and 500 000×, respectively. The bending of the lattice planes, obvious in Fig. 1, has been removed. The geometric phase methodology has also been applied to the corrected images. Figure 5(c,d) correspond to the β_{yx} component of the corrected images. The vertical stripes in the distorted images are no longer present after correction of the images using this algorithm. The narrow

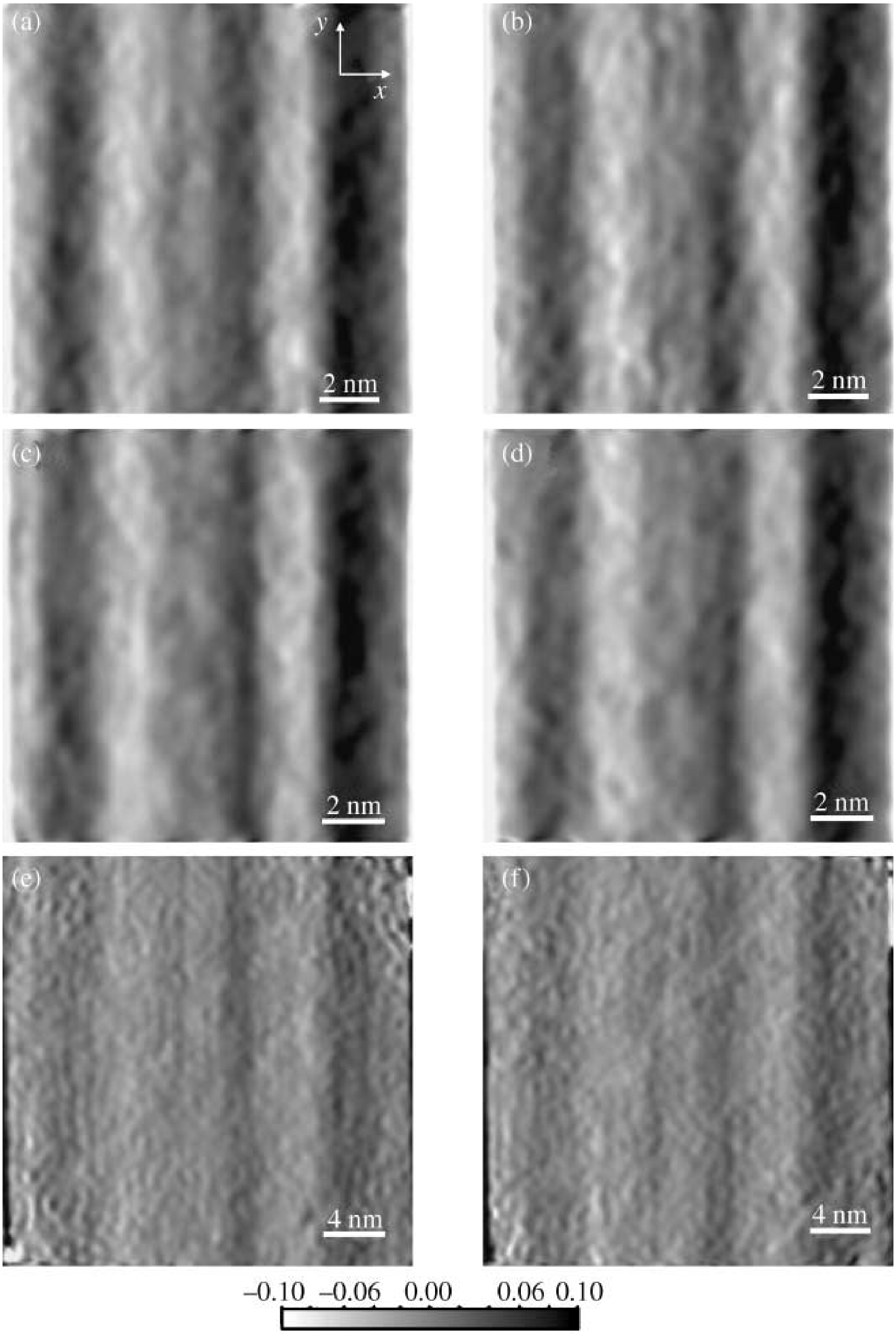

Fig. 3. Maps of β_{yx} from [110] GaAs recorded at (a–d) 1 000 000× and (e,f) 500 000× at different times.

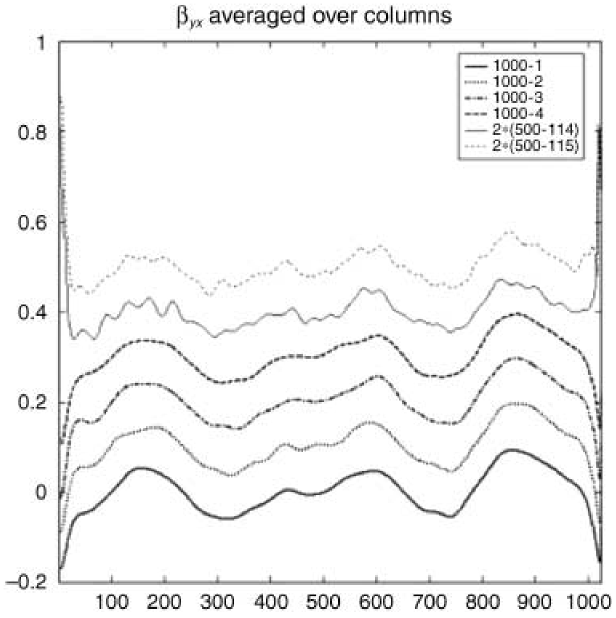

Fig. 4. Plots of β_{yx} using the average value of each column. The magnification is indicated as 1 000 (1 000 000×) and 500 (500 000×) in the key. Each curve has been displaced vertically by 0.1 for clarity.

horizontal lines visible in Fig. 1 do not introduce distortions and are still present in the corrected images.

Conclusions

In summary, we have shown that strain mapping can be used to measure systematic distortions in HAADF images, and the resulting strain values can be used to correct the images. Because the distortion was essentially the same for every image at a given magnification (i.e. 'systematic'), using a simple procedure we can quantify and remove the distortion. This result is very useful because it makes it possible to compare experimental and simulated HAADF images in order to determine the crystallography and defect structure.

Acknowledgements

A.M.S., M.F. and P.J.G. would like to acknowledge financial support from EPSRC for many aspects of this programme of work.

References

Beanland, R. (2003) Rapid cross-section TEM specimen preparation of III–V materials. *Microscopy Today*, **11**, 29–31.

Bierwolf, R., Hohenstein, M., Phillipp, F., Brandt, O., Crook, G.E. & Ploog, K. (1993) Direct measurement of local lattice-distortions in strained layer structures by HREM. *Ultramicroscopy*, **49**, 273–285.

Galindo, P.L., Yañez, A., Pizarro, J., Guerrero, E., Ben, T. & Molina, S.I. (2005) Strain mapping from HRTEM images. *Proceedings of the MSM XIV Conference*. IOP, Oxford, in press.

Hÿtch, M.J. & Plamann, T. (2001) Imaging conditions for reliable measurement of displacement and strain in high-resolution electron microscopy. *Ultramicroscopy*, **87**, 199–212.

Hÿtch, M.J., Snoeck, E. & Kilaas, R. (1998) Quantitative measurement of displacement and strain fields from HREM micrographs. *Ultramicroscopy*, **74**, 131–146.

Kret, S., Ruterana, P., Rosenauer, A. & Gerthsen, D. (2001) Extracting quantitative information from high resolution electron microscopy. *Phys. Stat. Sol. (B)*, **227**, 247–295.

Krivanek, O.L., Dellby, N. & Lupini, A.R. (1999) Towards sub-angstrom electron beams. *Ultramicroscopy*, **78**, 1–11.

Rosenauer, A., Remmele, T., Gerthsen, D., Tillmann, K. & Förster, A. (1997) Atomic scale strain measurements by the digital analysis of transmission electron microscopic lattice images. *Optik*, **105**, 99–107.

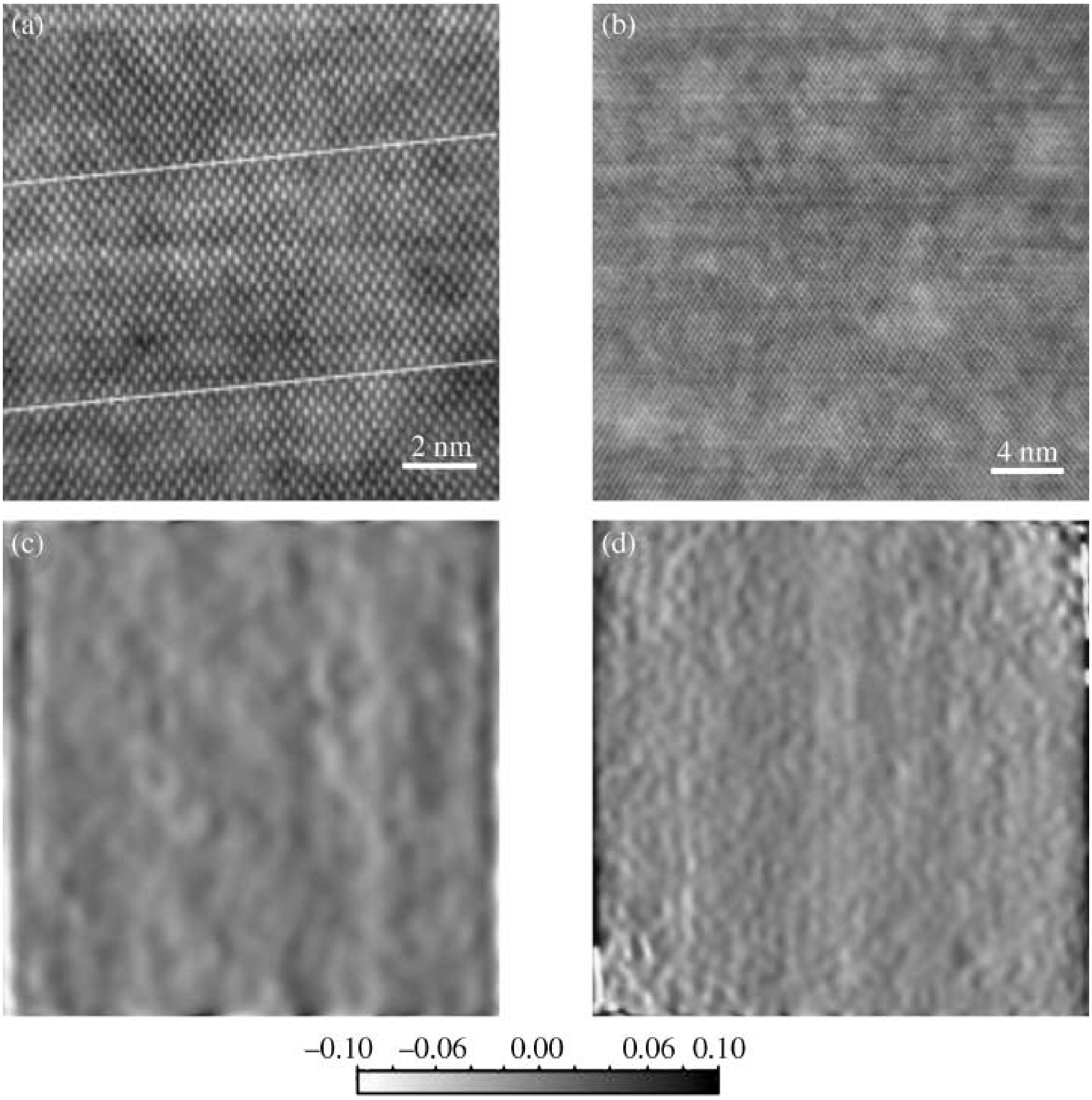

Fig. 5. Corrected High-angle annular dark-field image at (a) 1 000 000× and (b) 500 000×. The β_{yx} component of the distortion tensor corresponding to (a) and (b) is shown in (c) and (d), respectively. Two white lines were drawn in (a) to highlight the straight lattice planes after the correction of systematic distortion.